

# Journal of Visualized Experiments

## Imaging mitochondrial Ca<sup>2+</sup> uptake in astrocytes and neurons using genetically encoded Ca<sup>2+</sup> indicators (GECIs) GCaMP5G/6s --Manuscript Draft--

<b>Article Type:</b>	Invited Results Article - Author Produced Video
<b>Manuscript Number:</b>	JoVE62917R4
<b>Full Title:</b>	Imaging mitochondrial Ca <sup>2+</sup> uptake in astrocytes and neurons using genetically encoded Ca <sup>2+</sup> indicators (GECIs) GCaMP5G/6s
<b>Corresponding Author:</b>	Shinghua Ding University of Missouri Columbia Columbia, MO UNITED STATES
<b>Corresponding Author's Institution:</b>	University of Missouri Columbia
<b>Corresponding Author E-Mail:</b>	dings@missouri.edu
<b>Order of Authors:</b>	Shinghua Ding Nannan Zhang Zhe Zhang Ilker Ozden
<b>Additional Information:</b>	
<b>Question</b>	<b>Response</b>
Please specify the section of the submitted manuscript.	Neuroscience
Please indicate whether this article will be Standard Access or Open Access.	Standard Access (\$1400)
Please confirm that you have read and agree to the terms and conditions of the author license agreement that applies below:	I agree to the <a href="#">Author License Agreement</a>
Please provide any comments to the journal here.	
Please confirm that you have read and agree to the terms and conditions of the video release that applies below:	I agree to the <a href="#">Video Release</a>

**TITLE:**

Imaging Mitochondrial  $\text{Ca}^{2+}$  Uptake in Astrocytes and Neurons using Genetically Encoded  $\text{Ca}^{2+}$  Indicators (GECIs)

**AUTHORS AND AFFILIATIONS:**

Nannan Zhang<sup>1</sup>, Zhe Zhang<sup>1,2</sup>, Ilker Ozden<sup>2</sup>, Shinghua Ding<sup>1,2</sup>

<sup>1</sup>Dalton Cardiovascular Research Center, University of Missouri-Columbia, MO

<sup>2</sup>Department of Biomedical, Biological and Chemical Engineering, University of Missouri-Columbia, MO

**Email Addresses of Co-authors:**

Nannan Zhang ([Zhangn@missouri.edu](mailto:Zhangn@missouri.edu))

Zhe Zhang ([zz8wd@mail.missouri.edu](mailto:zz8wd@mail.missouri.edu))

Ilker Ozden ([ozdeni@missouri.edu](mailto:ozdeni@missouri.edu))

Shinghua Ding ([dings@missouri.edu](mailto:dings@missouri.edu))

**Email address of corresponding author:**

Shinghua Ding ([dings@missouri.edu](mailto:dings@missouri.edu))

**KEYWORDS:**

astrocyte, neuron, mitochondria, GECIs, GCaMP5G/6s, mitochondria-targeting sequence, gfaABC1D promoter, CaMKII promoter, *in vivo* 2-photon imaging

**SUMMARY:**

This protocol aims to provide a method for *in vitro* and *in vivo* mitochondrial  $\text{Ca}^{2+}$  imaging in astrocytes and neurons.

**ABSTRACT:**

Mitochondrial  $\text{Ca}^{2+}$  plays a critical role in controlling cytosolic  $\text{Ca}^{2+}$  buffering, energy metabolism, and cellular signal transduction. Overloading of mitochondrial  $\text{Ca}^{2+}$  contributes to various pathological conditions, including neurodegeneration and apoptotic cell death in various neurological diseases. Here we present a cell-type specific and mitochondria targeting molecular approach for mitochondrial  $\text{Ca}^{2+}$  imaging in astrocytes and neurons *in vitro* and *in vivo*. We constructed DNA plasmids encoding mitochondria-targeting genetically encoded  $\text{Ca}^{2+}$  indicators (GECIs) GCaMP5G or GCaMP6s (GCaMP5G/6s) with astrocyte- and neuron-specific promoters gfaABC1D and CaMKII and mitochondria-targeting sequence (mito-). For *in vitro* mitochondrial  $\text{Ca}^{2+}$  imaging, the plasmids were transfected in cultured astrocytes and neurons to express GCaMP5G/6s. For *in vivo* mitochondrial  $\text{Ca}^{2+}$  imaging, adeno-associated viral vectors (AAVs) were prepared and injected into the mouse brains to express GCaMP5G/6s in mitochondria in astrocytes and neurons. Our approach provides a useful mean to image mitochondrial  $\text{Ca}^{2+}$  dynamics in astrocytes and neurons to study the relationship between cytosolic and mitochondrial  $\text{Ca}^{2+}$  signaling, as well as astrocyte-neuron interactions.

**INTRODUCTION:**

Mitochondria are dynamic subcellular organelles and are considered as the cell powerhouses for energy production. On the other hand, mitochondria can take up  $\text{Ca}^{2+}$  in the matrix in response to local or cytosolic  $\text{Ca}^{2+}$  rises. Mitochondrial  $\text{Ca}^{2+}$  uptake affects mitochondrial function, including metabolic processes such as reactions in the tricarboxylic acid (TCA) cycle and oxidative phosphorylation, and regulates  $\text{Ca}^{2+}$ -sensitive proteins under physiological conditions<sup>1-4</sup>. Mitochondrial  $\text{Ca}^{2+}$  overloading is also a determinant for cell death, including necrosis and apoptosis in various brain disorders<sup>5-7</sup>. It causes the opening of mitochondrial permeability transition pores (mPTPs) and the release of caspase cofactor, which initiate apoptotic cell death. Therefore, it is important to study mitochondrial  $\text{Ca}^{2+}$  dynamics and handling in living cells to understand cellular physiology and pathology better.

Mitochondria maintain matrix  $\text{Ca}^{2+}$  homeostasis through a balance between  $\text{Ca}^{2+}$  uptake and efflux. Mitochondrial  $\text{Ca}^{2+}$  uptake is mainly mediated by mitochondrial  $\text{Ca}^{2+}$  uniporters (MCUs), while mitochondrial  $\text{Ca}^{2+}$  efflux is mediated by the  $\text{Na}^+$ - $\text{Ca}^{2+}$ - $\text{Li}^+$  exchangers (NCLXs) and the  $\text{H}^+$ / $\text{Ca}^{2+}$  exchangers (mHCXs)<sup>8</sup>. The balance can be perturbed through the stimulation of G-protein coupled receptors (GPCRs)<sup>9</sup>. Mitochondrial  $\text{Ca}^{2+}$  homeostasis is also affected by mitochondrial buffering by the formation of insoluble  $\text{xCa}^{2+}$ - $\text{xPO}_4\text{x}$ - $\text{xOH}$  complexes<sup>8</sup>.

Intracellular and mitochondrial changes in  $\text{Ca}^{2+}$  concentration ( $[\text{Ca}^{2+}]$ ) can be evaluated by fluorescent or luminescent  $\text{Ca}^{2+}$  indicators.  $\text{Ca}^{2+}$  binding to indicators causes spectral modifications, allowing to recording of free cellular  $[\text{Ca}^{2+}]$  in real-time in live cells. Two types of probes are currently available to monitor  $\text{Ca}^{2+}$  changes in cells: organic chemical indicators and genetically-encoded  $\text{Ca}^{2+}$  indicators (GECIs). Generally, different variants with different  $\text{Ca}^{2+}$  affinities (based on  $K_d$ ), spectral properties (excitation and emission wavelengths), dynamic ranges, and sensitivities are available for the biological questions under investigation. Although many synthetic organic  $\text{Ca}^{2+}$  indicators have been used for cytosolic  $\text{Ca}^{2+}$  imaging, only a few can be selectively loaded in the mitochondrial matrix for mitochondrial  $\text{Ca}^{2+}$  imaging, with Rhod-2 being the most widely used (for reviews see<sup>10,11</sup>). However, Rhod-2 has a major drawback of leakage during long time-course experiments; in addition, it is partitioned between mitochondria, other organelles and the cytosol, making absolute measurements in different subcompartments difficult. In contrast, by using cell-type specific promoters and subcellular compartment targeting sequences, GECIs can be expressed in different cell types and subcellular compartments for cell- and compartment-specific  $\text{Ca}^{2+}$  imaging *in vitro* or *in vivo*. Single-wavelength fluorescence intensity-based GCaMP  $\text{Ca}^{2+}$  indicators have recently emerged as major GECIs<sup>12-16</sup>. In this article, we provide a protocol for mitochondria-targeting and cell-type specific expression of GCaMP5G and GCaMP6s (GCaMP5G/6s) in astrocytes and neurons, and imaging mitochondrial  $\text{Ca}^{2+}$  uptake in astrocytes and neurons. Using this protocol, the expression of GCaMP6G/6s in individual mitochondria can be revealed and  $\text{Ca}^{2+}$  uptake in single mitochondrial resolution can be achieved in astrocytes and neurons *in vitro* and *in vivo*.

## PROTOCOL:

Procedures involving animals have been approved by the Institutional Animal Care and Use Committee (IACUC) at the University of Missouri-Columbia.

## 1. Construction of DNA plasmids

NOTE: For *in vitro* and *in vivo* imaging, DNA plasmid with astrocyte- and neuron-specific promoters encoding GCaMP5G/6s are constructed with mitochondrial targeting sequences.

1.1. Insert mitochondrial matrix (MM)-targeting sequence (mito-) ATGT CCGTCCTGAC GCCGCTGCTG CTGCGGGGCT TGACAGGCTC GGCCCGGCGG CTCCCAGTGC CGCGCGCCAA GATCCATTCG TTG<sup>17</sup> into the cloning sites EcoRI and BamHI in the backbone of adeno-associated virus (AAV) plasmid pZac2.1 to obtain plasmids containing astrocytic gfaABC<sub>1</sub>D promoter or neuronal CaMKII promoter<sup>18–20</sup>.

1.2. Subclone GCaMP5G/6s into the cloning sites BamH I and Not 1 in the above plasmids to obtain new plasmids pZac-gfaABC1D-mito-GCaMP5G/6s and pZac-CaMKII-mito-GCaMP5G/6s that target transgene expression in mitochondria in astrocytes and neurons<sup>20,21</sup> (**Figure 1A**).

1.3. Prepare pZac-gfaABC1D-mito-GCaMP5G and pZac-CaMKII-mito-GCaMP6s DNA plasmids for transfection for *in vitro* study (Section 2). Produce AAV vectors with serotype 5 for astrocytes and serotype 9 for neurons for *in vivo* study<sup>18</sup> (Section 3).

## 2. *In vitro* mitochondrial Ca<sup>2+</sup> imaging in astrocytes and neurons

2.1. Prepare primary astrocytes from the cortex of P1 neonatal mice and primary neurons from the cortex of E15–16 embryos<sup>18,22–24</sup>, and culture them on 12 mm diameter glass coverslips in 24-well plates using Dulbecco's Modified Eagle Medium (DMEM) containing 10% fetal bovine serum (FBS), and neuronal basal medium (NBM) containing 2% B27, respectively.

2.2. Transfect mature astrocytes and neurons with pZac-gfaABC1D-GCaMP6s and pZac-CaMKII-GCaMP5G plasmids using lipid based transfection reagent to express GCaMP6s in the mitochondria of astrocytes and GCaMP5G in the mitochondria of neurons<sup>18,20,21</sup>. Transfect cells in each well with 0.5 µg of DNA, and change the medium 6 h later.

NOTE: The astrocytes and neurons are ready for imaging 1–2 days after transfection.

2.3. Perform *in vitro* mitochondrial Ca<sup>2+</sup> imaging 1–2 days after transfection.

2.3.1. Transfer the glass coverslips cultured with astrocytes or neurons to the PH-1 perfusion chamber under an epifluorescence or two photon microscope.

2.3.2. Stimulate astrocytic mitochondrial Ca<sup>2+</sup> uptake with 100 µM ATP in ACSF, or stimulate neuronal mitochondria with 100 µM glutamate/10 µM glycine<sup>20,25</sup> (**Figure 2** and **Figure 3**).

NOTE: Solution changes from ACSF to ATP- and glutamate/glycine-containing ACSF are controlled by an ALA-VM8 perfusion system<sup>21</sup>. The speed of the solution change is controlled at 1–2 mL/min by adjusting a valve.

### 3. *In vivo* mitochondrial Ca<sup>2+</sup> imaging in astrocytes and neurons

#### 3.1. AAV preparations.

3.1.1. Prepare the following recombinant adeno-associated virus (rAAV) vectors using the DNA plasmids prepared in section 1: rAAV2/5-gfaABC1D-mito-GCaMP5G and rAAV2/9-CaMKII-mito-GCaMP6s vectors.

NOTE: In this experiment, rAAV vectors of serotype 5 were prepared to express GCaMP5G in mitochondria in astrocytes and rAAV vectors of serotype 9 were prepared to express GCaMP6s in mitochondria for neurons.

#### 3.2. Stereotaxic AAV injection.

3.2.1. Anesthetize the mouse with 3% isoflurane.

NOTE: Later during the surgery, the isoflurane levels are reduced to 2%.

3.2.2. After the mouse reaches a surgical level of anesthesia, as determined by tail and toe pinch, shave the hair over the surgery site, motor or somatosensory cortex, with a hair trimmer.

3.2.3. Position the mouse on the mouse stereotaxic device and fix the head with ear bars. Apply ophthalmic ointment to the eyes to protect them during the surgery. Use a heating pad to keep the body temperature of the mouse at 37 °C throughout the surgery.

NOTE: Perform surgery using aseptic procedures. All surgical tools need to be sterilized either by autoclaving or using a hot bead sterilizer.

3.2.4. After the mouse is mounted on the stereotaxic device, sterilize the scalp with alternating iodine based scrub and 70% ethanol three times. Make an incision in the midline of the scalp to expose the injection site.

3.2.5. Cut open the skin in the bregma lamda axis and create a ~1 mm diameter burr hole with a high speed drill at the intended injection location of motor or somatosensory cortex.

3.2.6. Use a 33 G Hamilton syringe containing associated adenovirus (rAAV2/5-gfaABC1D-mito-GCaMP5G vectors [1 x 10<sup>11</sup> GC] and rAAV2/9-CaMKII-mito-GCaMP6s vectors [1 x 10<sup>11</sup> GC]) into the walls of mouse target area to inject upto 1 µL of vectors at the target area.

NOTE: For example, for cortical viral delivery, inject the virus solution at two depths in multiple steps. First insert the needle upto 1 mm depth and allow 5 min for the brain to recover. Then, move the needle up to ~700 µm depth and inject 500 nL of the virus solution at an injection speed of 10 nL/s using a hamilton syringe controlled by a microsyringe pump controller. After the injection is completed, wait for 5 min to allow the virus to diffuse into the brain. Then, move the needle up to the second injection location upto a depth of 300 µm. Here, inject an additional 500

nL of the virus solution. Wait for 10 min to allow th virus to diffuse into the brain.

3.2.7. Close the scalp and the skin using a tissue adhesive. Let the mice recover on the heating pad. Send mice back to the animal facility after recovery.

3.3. Cranial-window intstallation and *in vivo* 2-P imaging of mitochondrial  $\text{Ca}^{2+}$  signals.

NOTE: Cranial window implantation is done 3 weeks post AAV injection over the motor or somatosensory cortex<sup>26–29</sup>. Subcutaneous injection of carprofen (10 mg/Kg) is injected to provide relief from potential pain before surgery. The cranial window surgical procedures are identical to the AAV injection surgical procedures and are performed under aseptic conditions.

3.3.1. Anesthetize the mouse with 3% isoflurane.

NOTE: This is the initial dose and reduce to 2% for the surgery later on. During imaging, an intraperitoneal (IP) injection of 130 mg ketamine/10 mg xylazine/kg body weight dissolved in ACSF during imaging.

3.3.2. Position the mouse on the mouse stereotaxic device and fix the head with ear bars. Apply ophthalmic ointment to eyes. Use a heating pad to keep the body temperature of the mouse at 37 °C throughout the surgery.

NOTE: All surgical tools need to be sterilized.

3.3.3. Make an incision of 5–8 mm long in the midline of the scalp and remove a flap of skin using a pair of scissors.

3.3.4. After skull is exposed, perform 2.0–3.0 mm diameter craniotomy using a high-speed drill over the virus injected area (i.e., motor cortex or somatosensory cortex, **Figure 1B**). First make four small holes, and then drill along in a circle connecting the holes. Then, lift the bone with sharp scissors and remove. The exposed duramater can be removed or kept intact for impantation of the cranial window.

3.3.5. Place a glass coverslip of 3–5 mm in diameter carrying a transparent silicone over the craniotomy. Use a toothpick to push the cranial window gently onto the surface of the brain. Then, seal the edge with a small amount of silicone adhesive.

NOTES: Alternatively, instead of silicone disk, 1.2% low melting point agarose gel can be used between the cover glass and the brain tissue.

3.3.6. Finally, seal the edges of the coverslip with dental cement. Take care to apply the cement slightly at the edge of the dental window for strong bonding. Attach a custom-made metal head plate to the skull with cyanoacrylate glue.

NOTE: The metal plate is used to fix the head of the mouse to the stage of 2-P microscope during

the imaging session (**Figure 1C**).

3.3.7. Add 0.5 mL of ACSF solution over the coverslip on the cranial window.

3.3.8. Perform time-lapse *in vivo* 2-P imaging of mito-GCaMP5G in astrocyte and mito-GCaMP6s in neurons with 910 nm wavelength through the cranial window (**Figure 1C**)<sup>18,20,27</sup>.

NOTE: During imaging, mice are on the heating pad to maintain physiological temperature. The mice will be sacrificed immediately after the imaging session is completed.

3.3.9. Label astrocytes *in vivo* with sulforhodamine 101 (SR101) when it is necessary to determine colocalization.

3.3.9.1. At end of step 3.3.4, apply 100  $\mu$ L of 100  $\mu$ M SR101 in ACSF on the cortical surface for 1–5 min.

3.3.9.2. Rinse the surface with ACSF to wash away the unbound SR101. Using 2-P imaging, co-labeling of mito-GCaMP5G and SR101 in astrocytes can be observed 45–60 min later (**Figure 4A**).

## REPRESENTATIVE RESULTS:

The aim of this study was to provide methodology to image mitochondrial  $\text{Ca}^{2+}$  signal using GECIs in astrocytes and neurons *in vitro* and *in vivo*. Results of both *in vitro* and *in vivo* mitochondrial  $\text{Ca}^{2+}$  imaging are presented here.

### ***In vitro* mitochondrial $\text{Ca}^{2+}$ signaling in cultured astrocytes and neurons**

Mitochondrial  $\text{Ca}^{2+}$  uptake in astrocytes can be elicited by ATP application, and mitochondrial  $\text{Ca}^{2+}$  uptake in neurons can be elicited by glutamate and glycine application through a perfusion system. **Figure 2** and **Figure 3** show GCaMP6s is expressed in cultured astrocytes and GCaMP5G in neurons, respectively. Mitochondrial  $\text{Ca}^{2+}$  uptake in astrocytes was elicited by 100  $\mu$ M ATP with individual mitochondrial resolution (**Figure 2B–D**). Mitochondrial  $\text{Ca}^{2+}$  uptakes in neurons was elicited by 100  $\mu$ M glutamate and 10  $\mu$ M glycine with individual mitochondrial resolution (**Figure 3B–D**).

### ***In vivo* 2-P imaging of mitochondrial expression of GCaMP5G or 6S in astrocytes and neurons**

The imaging is done by collecting time-lapse *in vivo* 2-P imaging of mitochondrial fluorescence signals in astrocytes and neurons with an Ultima 2-P microscope system. We use excitation wavelength 880–910 nm. **Figure 4** shows expression of GCaMP5G in mitochondria in astrocytes in the mouse cortex. The astrocyte-specific expression of GCaMP5G was confirmed by colocalization of SR101 with GCaMP5G with individual mitochondria resolution (**Figure 4A**), and spontaneous  $\text{Ca}^{2+}$  changes in individual mitochondria can be observed (**Figure 4B–E**). **Figure 5A** shows neuron-specific expression of mito-GCaMP6s colocalized with neuronal marker NeuN. The fluorescence of mito-GCaMP6s in neurons shows mitochondrial morphology in dendrites (**Figure 5B**). Spontaneous mitochondrial  $\text{Ca}^{2+}$  increases in dendrites can be observed (**Figure 5C–F**).

## Analysis of mitochondrial $\text{Ca}^{2+}$ signals

Quantify the fluorescent signals by calculating the mean pixel intensities of the cell body or individual mitochondria in astrocytes and neurons using image analysis software.  $\text{Ca}^{2+}$  changes overtime (t) are expressed as  $\Delta\text{F}/\text{Fo}$  (t) values versus time, where  $\text{Fo}$  is the background subtracted baseline fluorescence and  $\Delta\text{F}$  is the baseline subtracted fluorescence change<sup>20,21</sup>. Use the peak  $\Delta\text{F}/\text{Fo}$  values to compare the amplitude of  $\text{Ca}^{2+}$  signals.

### FIGURE LEGENDS:

**Figure 1: DNA constructs for astrocyte- and neuron-specific and mitochondria-targeting transgene expression, and *in vivo* 2-P imaging.** (A) DNA Constructs of genetically encoded  $\text{Ca}^{2+}$  indicator GCaMP5G or GCaMP6s in pZac2.1 plasmid with gfaABC<sub>1</sub>D (up) and CaMKII (low) promoters for delivery to astrocytic and neuronal mitochondrial matrix, respectively. Mitochondria-targeting is achieved using a mitochondrial matrix (MM) specific sequence (mito) appended to the N-terminus of the fluorescent proteins. (B) A craniotomy over the cortex of a mouse. (C) The skull of a mouse is attached to a metal plate connected to the post fixed on the stage of 2-P microscope. The inset shows the cranial window with a metal plate attached to the skull.

**Figure 2: Mitochondrial  $\text{Ca}^{2+}$  imaging of cultured astrocytes.** (A–B) A 2-P image of an astrocyte expressing mito-GCaMP6s (A) and its response to the stimulation of 100  $\mu\text{M}$  ATP at the indicated time (B). (C) Images of mito-GCaMP6s in the four individual mitochondria (in A, circles) at the different times after ATP stimulation. (D) The time courses of mito-GCaMP6s fluorescence changes, plotted as  $\Delta\text{F}/\text{Fo}$ , in the four individual mitochondria after ATP stimulation. The red arrow indicates the starting time of imaging. The pseudocolor scale is a linear representation of the fluorescence intensity in this and other figures.

**Figure 3: Mitochondrial  $\text{Ca}^{2+}$  imaging of cultured neurons.** (A–B) A 2-P images of mito-GCaMP5G expressing neuron (A) and its response to 100  $\mu\text{M}$  glutamate at the indicated times (B). (C) Images of mito-GCaMP5G in the four individual mitochondria (in A, circles) at different times after glutamate stimulation. (D) The time courses of mito-GCaMP5G fluorescence changes in the four individual mitochondria.

**Figure 4: *In vivo* 2-P imaging of mitochondrial  $\text{Ca}^{2+}$  signaling in astrocytes.** (A) 2-P images of mito-GCaMP5G expressing astrocytes colocalized with SR101. (B–C) 2-P image of an astrocyte expressing mito-GCaMP5G for analysis of spontaneous  $\text{Ca}^{2+}$  increase. (C–E) Images of mito-GCaMP5G in the four individual mitochondria in the astrocyte (in B, circles) at the different times (C) and the time courses of mito-GCaMP5G fluorescence changes, plotted as  $\Delta\text{F}/\text{Fo}$ , in the four individual mitochondria (E).

**Figure 5: *In vivo* 2-P imaging of mitochondrial  $\text{Ca}^{2+}$  signaling in neurons.** (A) Colocalization of GCaMP6s (upper) with neuronal marker NeuN (middle) in the brain. (B) High resolution images of dendrites expressing GCaMP6s with mitochondrial morphology (indicated by \*s). (C) GCaMP6s expressed in neuronal mitochondria. (D–F) Analysis of spontaneous mitochondrial  $\text{Ca}^{2+}$  increase in neurons. Pseudocolor 2-P image of the mitochondria expressing mito-GCaMP6s in C at



different times (**D**). Images of mito-GCaMP6s in the four individual mitochondria in C (circles) at the different times (**E–F**) and the time courses of mito-GCaMP6s fluorescence changes, plotted as  $\Delta F/F_0$ , in the four individual mitochondria (**F**).

**Movie: Mitochondrial  $\text{Ca}^{2+}$  increases based on GCaMP5G fluorescence changes in response to 100  $\mu\text{M}$  ATP in cultured astrocytes.**

## DISCUSSION:

In this article, we provide a method and protocol for imaging mitochondrial  $\text{Ca}^{2+}$  in astrocytes and neurons. We implemented mitochondria-targeting and cell type-specific strategies to express GECI GCaMP5G/6s. To target GCaMP5G/6s in mitochondria, we included a mitochondria-targeting sequence in the plasmids. To express GCaMP5G/6s in astrocytes and neurons *in vivo*, we inserted an astrocyte-specific promoter gfaABC1D and neuron-specific promoter CaMKII into the plasmids. Cell-type specific expression of GCaMP5G/6s in astrocytes and neurons can be confirmed by SR101 labeling in astrocytes and immunostaining of neurons with NeuN. From our data, these strategies provide a reliable cell type specific approach for mitochondrial  $\text{Ca}^{2+}$  imaging in astrocytes and neurons *in vivo*.

One potential problem for GECI expression is that it might cause  $\text{Ca}^{2+}$  buffering since it may reduce free  $\text{Ca}^{2+}$  by  $\text{Ca}^{2+}$  binding. Another problem that might be paid attention to is the amount of virus injected. Individual cells expressing GECI may not be identified if excessive virus is injected. These problems can be effectively ameliorated by reducing the titer of AAV. Photobleaching might also be an issue. Theoretically, all fluorescent indicators are subject to photobleaching. GCaMP5G/6s are quite stable, but they will bleach under continual exposure to excitation light. One general practice to avoid photobleaching is to reduce exposure time of tissue to laser light while ensuring enough fluorescence is collected. This can be achieved if high sensitivity PMTs and high light transmission objective are used. Photobleaching can also be reduced by closing shutter between images.

In our results of *in vivo* 2-P imaging, spontaneous mitochondrial increases can be observed both in astrocyte and neurons. Notably, these mitochondrial  $\text{Ca}^{2+}$  transients have long durations (**Figure 4E** and **Figure 5E**), consistent with a recent report by Gobel et al.<sup>30</sup>. The underlying mechanism of this phenomenon is not clear but is worth being pursued further. For cytosolic  $\text{Ca}^{2+}$  increase, astrocytes and neurons have different mechanisms. G-protein receptor stimulations cause  $\text{Ca}^{2+}$  increase in ER in astrocytes while the activations of voltage gated  $\text{Ca}^{2+}$  channels or glutamate receptors cause cytosolic  $\text{Ca}^{2+}$  increase in neurons, which can be uptaken by mitochondria. In our previous study<sup>20</sup>, we found that when mito-GCaMP5G was cotransfected with IP<sub>3</sub> 5-phosphatase (5ppase) cultured astrocytes, ATP-induced mitochondrial  $\text{Ca}^{2+}$  increase could be largely abolished. However, the two mutants of 5ppase, i.e., R343A and R343A/R350A 5ppase, which lack enzymatic activity, did not affect the mitochondrial  $\text{Ca}^{2+}$  increase after ATP stimulation. The results indicate that cytosolic and mitochondrial  $\text{Ca}^{2+}$  levels are highly coupled, likely because of the intimate physical connection between the ER and mitochondria in astrocytes, with the cytosol serving as an intermediary conduit for  $\text{Ca}^{2+}$  delivery. We also found that glutamate stimulation caused mitochondrial  $\text{Ca}^{2+}$  increase in neurons, suggesting glutamate receptors play a role in  $\text{Ca}^{2+}$  entry from extracellular space. In the future, it will be interesting to

study sensory-driven mitochondrial  $\text{Ca}^{2+}$  increases in astrocytes and neurons.

Our approach can be used to simultaneously image cytosolic and mitochondrial  $\text{Ca}^{2+}$  signals in the same cell type when two GECIs of different fluorescence wavelengths are expressed simultaneously, e.g., a red fluorescence GECI RCaMP in cytoplasm and GCaMP in mitochondria, or vice versa<sup>31</sup>. This approach can also be used for the *in vivo* study of astrocyte-neuron interactions in physiology and pathology with GCaMP expressed in astrocytes and RCaMP in neurons, or vice versa.

GCaMP is a GFP-based single fluorophore GECI. Currently, GCaMPs are the most preferred  $\text{Ca}^{2+}$  indicators because of their high signal-to-noise ratio (SNR), and large dynamic ranges (DR). Recently, jGCaMP7 sensors, the optimized version of GCaMP6, were reported with improved sensitivity to individual spikes<sup>16</sup>. GCaMP7 sensors can be easily subcloned in our plasmids for mitochondrial  $\text{Ca}^{2+}$  imaging. In summary, the strategies we presented here can be used to image mitochondrial  $\text{Ca}^{2+}$  uptake and handling in neurons and astrocytes with sufficient sensitivity to resolve  $\text{Ca}^{2+}$  changes at single mitochondrial level *in vivo*. This protocol represents a useful means to study cytosolic and mitochondrial  $\text{Ca}^{2+}$  signaling in astrocytes and neurons, as well as astrocyte-neuron interactions.

#### ACKNOWLEDGMENTS:

This work was supported by the National Institute of Health National Institute of Neurological Disorders and Stroke (NINDS) grants R01NS069726 and R01NS094539 to SD. We thank Erica DeMers for audio recording.

#### DISCLOSURES:

The authors have nothing to disclose.

#### REFERENCES:

1. Griffiths, E. J., Rutter, G. A. Mitochondrial calcium as a key regulator of mitochondrial ATP production in mammalian cells. *Biochimica et Biophysica Acta (BBA) - Bioenergetics*. **1787** (11), 1324–1333 (2009).
2. Pizzo, P., Drago, I., Filadi, R., Pozzan, T. Mitochondrial  $\text{Ca}^{2+}$  homeostasis: mechanism, role, and tissue specificities. *Pflugers Archiv - European Journal of Physiology*. **464** (1), 3–17 (2012).
3. Llorente-Folch, I. et al. Calcium-regulation of mitochondrial respiration maintains ATP homeostasis and requires ARALAR/AGC1-malate aspartate shuttle in intact cortical neurons. *The Journal of Neuroscience*. **33** (35), 13957–13971 (2013).
4. Burkeen, J. F., Womac, A. D., Earnest, D. J., Zoran, M. J. Mitochondrial calcium signaling mediates rhythmic extracellular ATP accumulation in suprachiasmatic nucleus astrocytes. *The Journal of Neuroscience*. **31** (23), 8432–8440 (2011).
5. Duchen, M. Mitochondria, calcium-dependent neuronal death and neurodegenerative disease. *Pflugers Archiv - European Journal of Physiology*. **464** (1), 111–121 (2012).
6. Gouriou, Y., Demareux, N., Bijlenga, P., De Marchi, U. Mitochondrial calcium handling during ischemia-induced cell death in neurons. *Biochimie*. **93** (12), 2060–2067 (2011).
7. Qiu, J. et al. Mitochondrial calcium uniporter Mcu controls excitotoxicity and is transcriptionally repressed by neuroprotective nuclear calcium signals. *Nature Communications*.

406 4, 2034 (2013).

407 8. Filadi, R., Greotti, E. The yin and yang of mitochondrial  $\text{Ca}^{2+}$  signaling in cell physiology  
408 and pathology. *Cell Calcium*. **93**, 102321 (2021).

409 9. Finkel, T. et al. The ins and outs of mitochondrial calcium. *Circulation Research*. **116** (11),  
410 1810–1819 (2015).

411 10. Paredes, R. M., Etzler, J. C., Watts, L. T., Zheng, W., Lechleiter, J. D. Chemical calcium  
412 indicators. *Methods*. **46** (3), 143–151 (2008).

413 11. Contreras, L., Drago, I., Zampese, E., Pozzan, T. Mitochondria: The calcium connection.  
414 *Biochimica et Biophysica Acta (BBA)*. **1797** (6–7), 607–618 (2010).

415 12. Tian, L. et al. Imaging neural activity in worms, flies and mice with improved GCaMP  
416 calcium indicators. *Nature Methods*. **6** (12), 875–881 (2009).

417 13. Yamada, Y. et al. Quantitative comparison of genetically encoded  $\text{Ca}^{2+}$  indicators in  
418 cortical pyramidal cells and cerebellar Purkinje cells. *Frontiers in Cellular Neuroscience*. **5**, 18  
419 (2011).

420 14. Akerboom, J. et al. Optimization of a GCaMP Calcium Indicator for Neural Activity Imaging.  
421 *The Journal of Neuroscience*. **32** (40), 13819–13840 (2012).

422 15. Chen, T. W. et al. Ultrasensitive fluorescent proteins for imaging neuronal activity. *Nature*.  
423 **499** (7458), 295–300 (2013).

424 16. Dana, H. et al. High-performance calcium sensors for imaging activity in neuronal  
425 populations and microcompartments. *Nature Methods*. **16** (7), 649–657 (2019).

426 17. Rizzuto, R., Brini, M., Pizzo, P., Murgia, M., Pozzan, T. Chimeric green fluorescent protein  
427 as a tool for visualizing subcellular organelles in living cells. *Current Biology: CB*. **5** (6), 635–642  
428 (1995).

429 18. Xie, Y., Wang, T., Sun, G. Y., Ding, S. Specific disruption of astrocytic  $\text{Ca}^{2+}$  signaling pathway  
430 in vivo by adeno-associated viral transduction. *Neuroscience*. **170** (4), 992–1003 (2010).

431 19. Lee, Y. et al. GFAP promoter elements required for region-specific and astrocyte-specific  
432 expression. *Glia*. **56** (5), 481–493 (2008).

433 20. Li, H. et al. Imaging of mitochondrial  $\text{Ca}^{2+}$  dynamics in astrocytes using cell-specific  
434 mitochondria-targeted GCaMP5G/6s: Mitochondrial  $\text{Ca}^{2+}$  uptake and cytosolic  $\text{Ca}^{2+}$  availability  
435 via the endoplasmic reticulum store. *Cell Calcium*. **56** (6), 457–466 (2014).

436 21. Zhang, N., Ding, S. Imaging of mitochondrial and cytosolic  $\text{Ca}^{2+}$  signals in cultured  
437 astrocytes. *Current Protocols in Neuroscience*. **82**, 2.29.1–2.29.11 (2018).

438 22. Bi, J., Li, H., Ye, S. Q., Ding, S. Pre-B-cell colony-enhancing factor exerts a neuronal  
439 protection through its enzymatic activity and the reduction of mitochondrial dysfunction in in  
440 vitro ischemic models. *Journal of Neurochemistry*. **120** (2), 334–346 (2012).

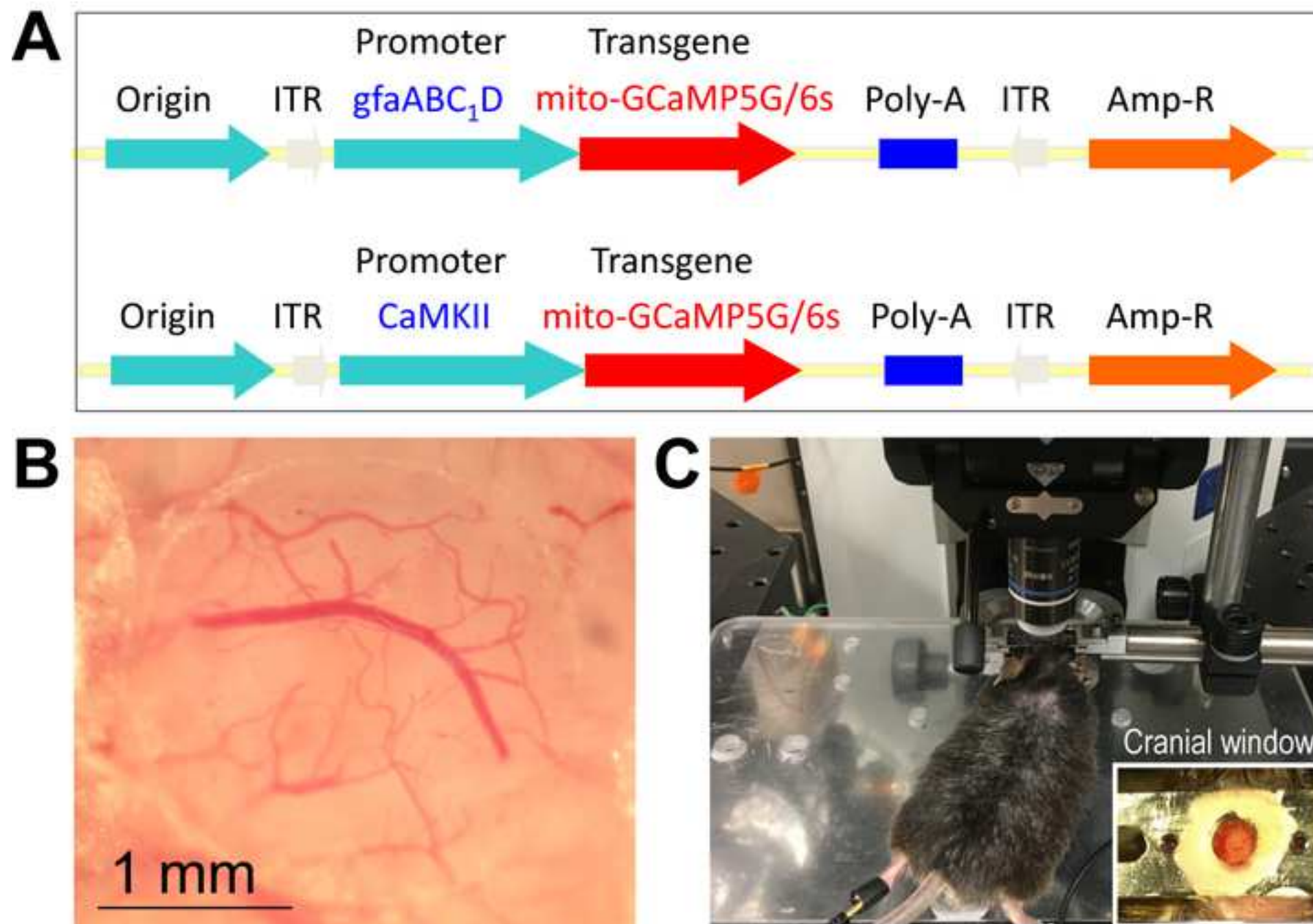
441 23. Wang, X., Li, H., Ding, S. Pre-B-cell colony-enhancing factor protects against apoptotic  
442 neuronal death and mitochondrial damage in ischemia. *Scientific Reports*. **6**, 32416 (2016).

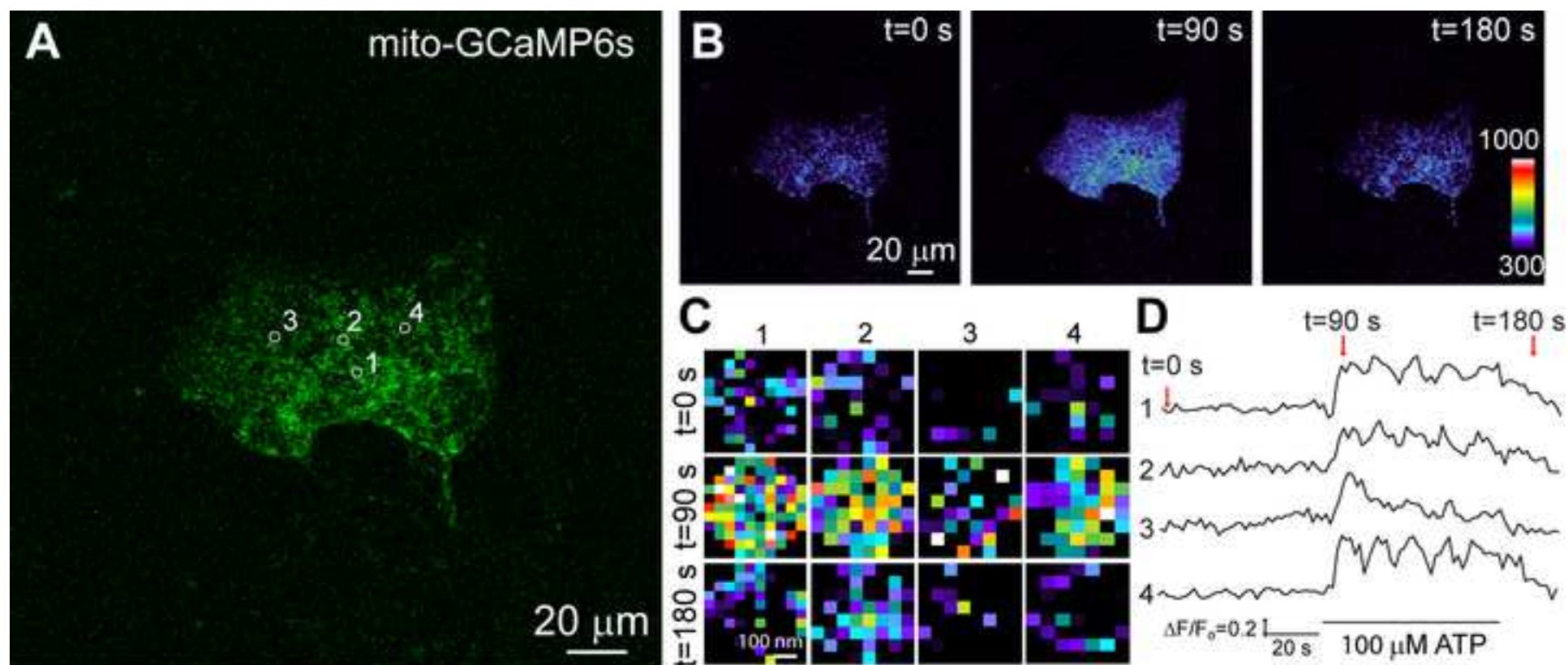
443 24. Wang, X. et al. Subcellular NAMPT-mediated  $\text{NAD}^+$  salvage pathways and their roles in  
444 bioenergetics and neuronal protection after ischemic injury. *Journal of Neurochemistry*. **151** (6),  
445 732–748 (2019).

446 25. Xie, Y., Chen, S., Wu, Y., Murphy, T. H. Prolonged deficits in parvalbumin neuron  
447 stimulation-evoked network activity despite recovery of dendritic structure and excitability in the  
448 somatosensory cortex following global ischemia in mice. *The Journal of Neuroscience*. **34** (45),  
449 14890–14900 (2014).

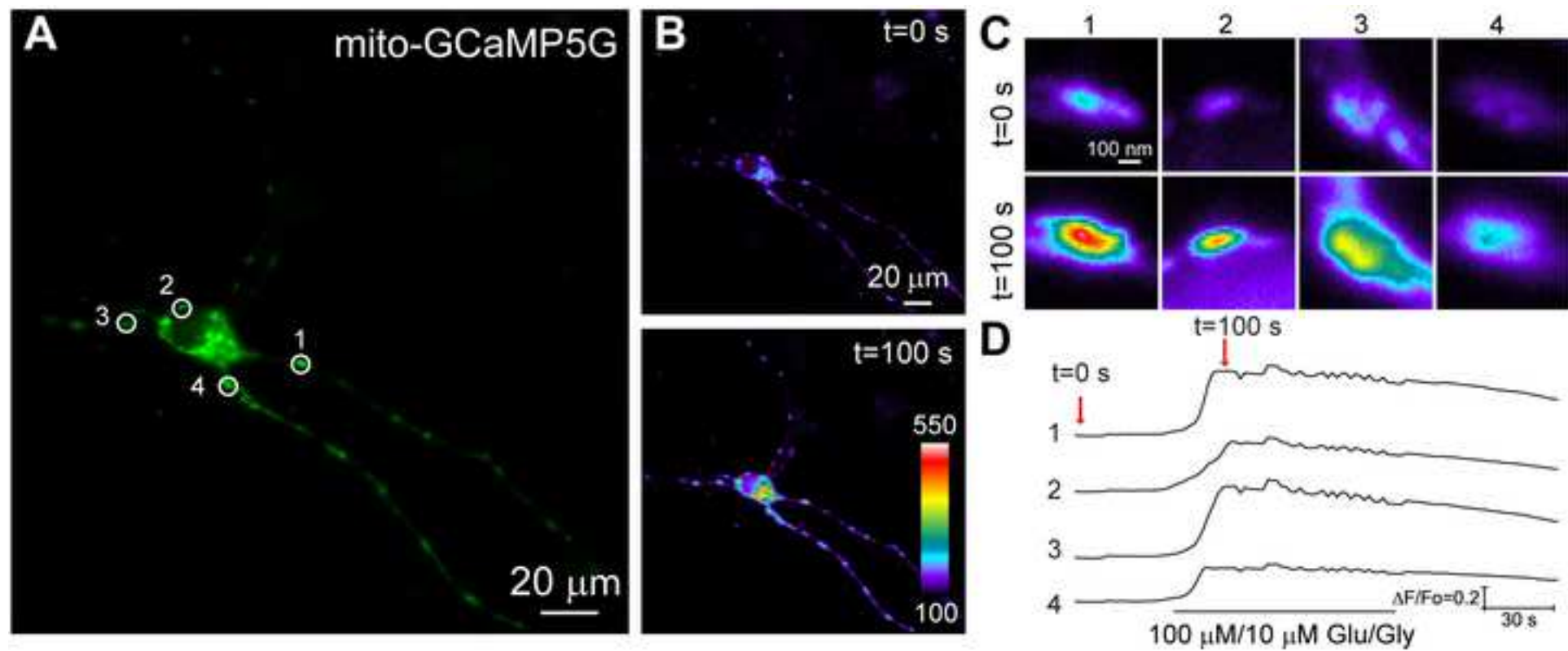
450 26. Ding, S. In vivo imaging of  $\text{Ca}^{2+}$  signaling in astrocytes using two-photon laser scanning

- fluorescent microscopy in *Astrocytes* (ed. Milner, R.) Humana Press. 545–554 (2012).
27. Li, H. et al. Disruption of IP<sub>3</sub>R2-mediated Ca<sup>2+</sup> signaling pathway in astrocytes ameliorates neuronal death and brain damage while reducing behavioral deficits after focal ischemic stroke. *Cell Calcium*. **58** (6), 565–576 (2015).
28. Ding, S. et al. Photothrombosis ischemia stimulates a sustained astrocytic Ca<sup>2+</sup> signaling in vivo. *Glia*. **57** (7), 767–776 (2009).
29. Ding, S. et al. Enhanced astrocytic Ca<sup>2+</sup> signals contribute to neuronal excitotoxicity after status epilepticus. *The Journal of Neuroscience*. **27** (40), 10674–10684 (2007).
30. Gobel, J. et al. Mitochondria-endoplasmic reticulum contacts in reactive astrocytes promote vascular remodeling. *Cell Metabolism*. **31** (4), 791–808 (2020).
31. Diaz-Garcia, C. M. et al. The distinct roles of calcium in rapid control of neuronal glycolysis and the tricarboxylic acid cycle. *eLife*. **10**, e64821 (2021).









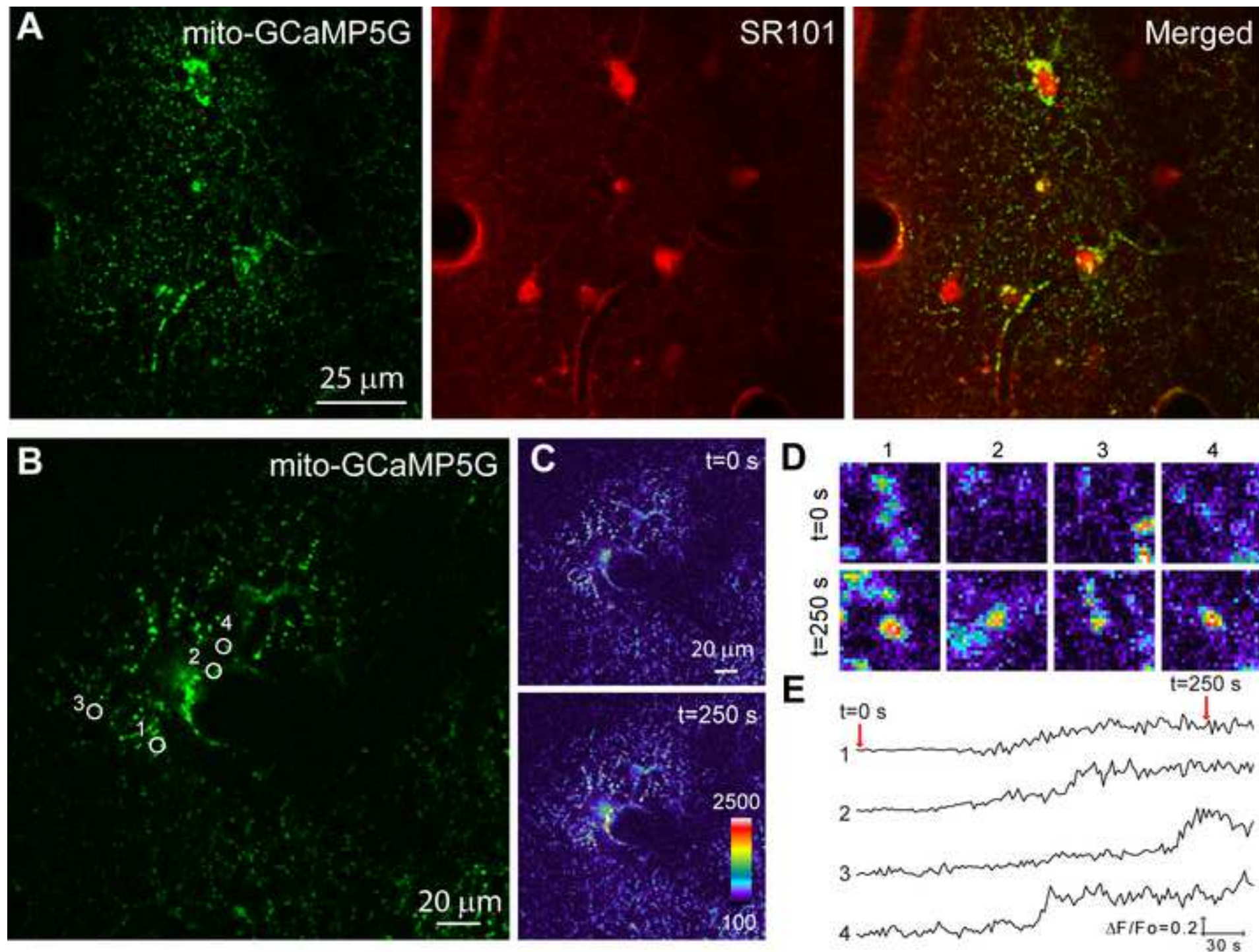
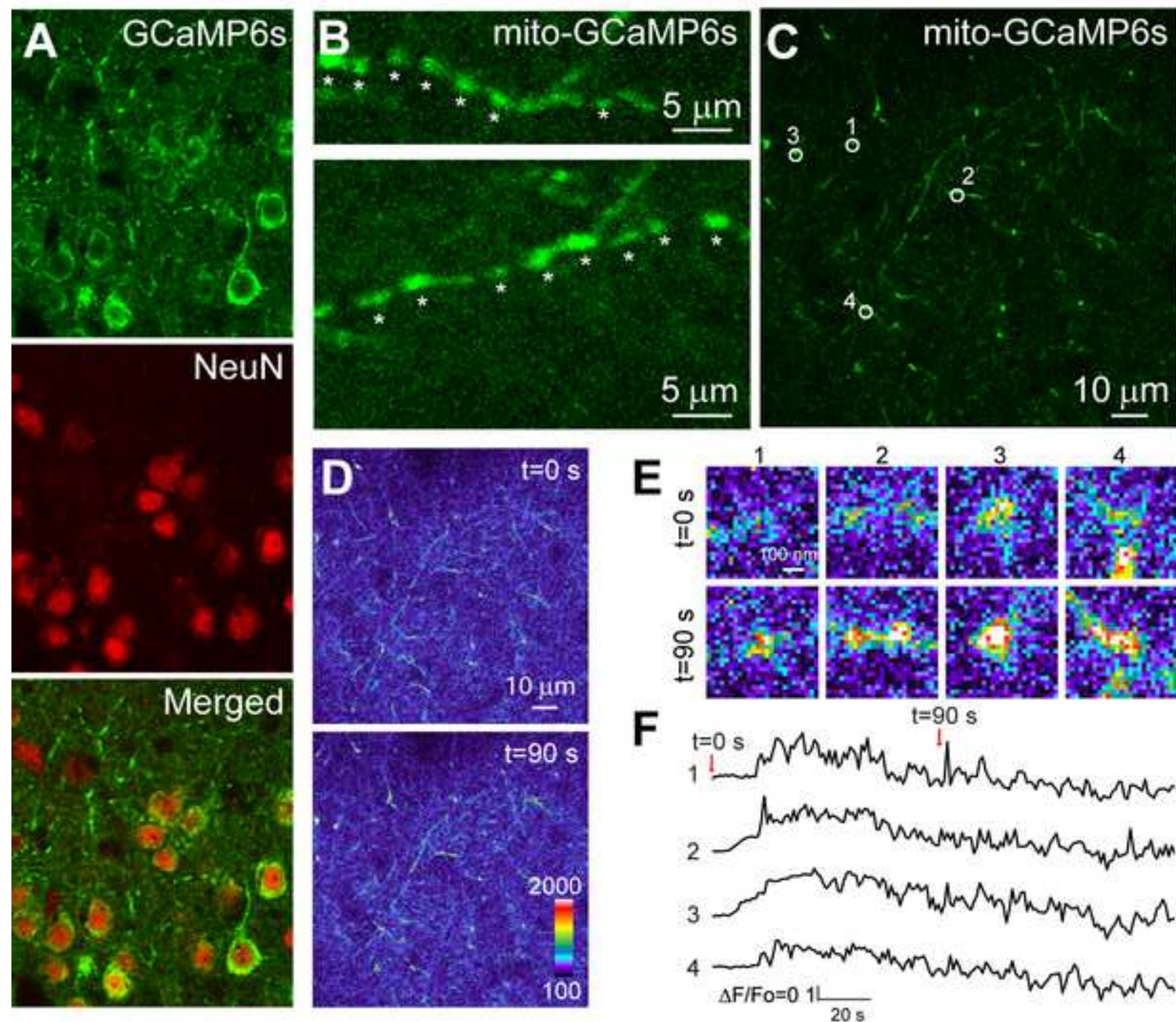




Figure 5



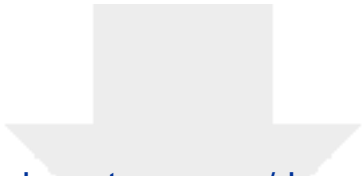


[Click here to access/download](#)

**Video or Animated Figure**

Mito-GCaMP6s\_cultured astrocyte\_JOVE.AVI

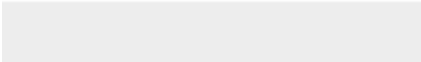




[Click here to access/download](#)

**Table of Materials**

Table of Materials\_revised.xlsx



Nov. 22, 2021

Dear Editor:

We thank you for rapid handling of our manuscript (62917R3, Imaging Mitochondrial  $\text{Ca}^{2+}$  Uptake in Astrocytes and Neurons using Genetically Encoded  $\text{Ca}^{2+}$  Indicators (GECIs)). We have addressed the editorial comments by cyan highlighted text so the text matches the video, and we also reply question in comments, while the yellow color from editorial editing remain unchanged. We also made minor editing of video. In addition, we made unsolicited changes of grammar in the text for proofread. We hope that this manuscript is now ready to be formally accepted for publication in your journal. Thank you very much for your attention.

Sincerely,



**Shinghua Ding, PhD**

Professor

Department of Biomedical, Biological and Chemical Engineering

Dalton Cardiovascular Research Center

Interdisciplinary Neuroscience Program (INP)

University of Missouri - Columbia

134 Research Park Drive

Columbia, MO 65211

Tel: (573) 884-2489 (O)

E-mail: [dings@missouri.edu](mailto:dings@missouri.edu)